

O VI Observations of the Onset of Convection Zones in Main-Sequence A Stars ¹

James E. Neff

Department of Physics & Astronomy, College of Charleston, Charleston, SC 29424

neffj@cofc.edu

and

Theodore Simon[†]

Institute for Astronomy, University of Hawaii, Honolulu, HI 96822

ABSTRACT

If magnetic activity in outer stellar atmospheres is due to an interplay between rotation and subsurface convection, as is generally presumed, then one would not expect to observe indicators of activity in stars with $T_{\text{eff}} \gtrsim 8300$ K. Any X-ray or ultraviolet line emission from hotter stars must be due either to a different mechanism or to an unresolved, active, binary companion. Due to their poor spatial resolution, X-ray instruments have been especially susceptible to source confusion. At wavelengths longward of $\text{Ly } \alpha$, the near ultraviolet spectra of stars hotter than this putative dividing line are dominated by photospheric continuum. We have used the *Far Ultraviolet Spectroscopic Explorer (FUSE)* to obtain spectra of the subcoronal O VI emission lines, which lie at a wavelength where the photospheric continuum of the mid- and early-A stars is relatively weak. We observed 14 stars spanning a range in T_{eff} from 7720 to 10,000 K. Eleven of the 14 stars showed O VI emission lines, including 6 of the 8 targets with $T_{\text{eff}} > 8300$ K. At face value, this suggests that activity does not fall off with increasing temperature. However, the emission lines are narrower than expected from the projected rotational velocities of these rapidly-rotating stars, suggesting that the emission could come from unresolved late-type companions. Furthermore, the strength of the O VI emission is consistent with that expected from

¹Based on observations made with the NASA-CNES-CSA *Far Ultraviolet Spectroscopic Explorer (FUSE)*, operated for NASA by the Johns Hopkins University under NASA contract NAS5-32985.

[†]Current Address: Eureka Scientific Inc., 1537 Kalaniewai Place, Honolulu HI 96821

an unseen active K or M dwarf binary companion, and the high $L_X/L(\text{O VI})$ ratios observed indicate that this must be the case. Our results are therefore consistent with earlier studies that have shown a rapid drop-off in activity at the radiative/convective boundary expected at $T_{\text{eff}} \sim 8300$ K, in agreement with conventional stellar structure models.

Subject headings: stars: activity — stars: chromospheres — stars: late-type — ultraviolet: stars

1. INTRODUCTION

The presence of 1–10 million-K coronae and 10–100 thousand-K chromospheres among all late-type stars, including the Sun, is generally accepted to be the direct result of stellar magnetism. Spatially-resolved observations of the solar surface, in fact, show a nearly linear correlation between X-ray brightness and magnetic flux that spans almost 12 orders of magnitude (Pevtsov et al. 2003). It is only in the case of the Sun, of course, that magnetic fields have actually been seen in ultraviolet (UV) and X-ray images of its outer atmosphere. For every other star, magnetic activity can at present only be inferred from spectral proxies, e.g., by the detection of UV emission lines or coronal X rays. It is also widely agreed that the origin of such activity among the dwarf stars of spectral types late-F through M lies deep within their interiors, through a dynamo process in which rotation interacts in an imperfectly understood way with turbulent convection. The process appears to operate most effectively in very young stars, which tend to rotate much more rapidly than the Sun, in very low-mass stars with very deep convection zones, and in short-period binaries where tidal interactions enforce rapid rotation by synchronizing the spin and orbital motions of the stars.

Whether magnetic dynamos of a similar nature operate in early-type stars and are able to power a hot chromosphere and corona in those objects remains an open question. The two most popular mechanisms for heating the outer layers of low-mass stars like the Sun—the dissipation of acoustic or magnetoacoustic waves, and microflaring of dynamo-generated turbulent magnetic fields—both require well-developed subsurface convection zones, which high-mass stars are thought to lack. According to stellar structure models, main-sequence A stars have vigorous convective cores, but the outer envelopes of those stars remain entirely radiative except for thin convective layers in the hydrogen and helium ionization zones at the base of the photosphere (Christensen-Dalsgaard 2000; Browning et al. 2004; Brun et al. 2005). The computational and theoretical challenge, then, is to show that magnetic fields generated by dynamo action within the convective core can rise to the surface on a time scale that is short compared with the main-sequence lifetime of such a star (MacGregor &

Cassinelli 2003; see, however, MacDonald & Mullan 2004) and that such a process indeed leads to the formation of a hot chromosphere and corona.

The possibility of dynamo activity in intermediate-mass and high-mass stars has been addressed by a variety of observations in recent years. Observations by the *International Ultraviolet Explorer (IUE)* and the *Hubble Space Telescope (HST)* at near-UV wavelengths have detected high-temperature chromospheric emission lines as far up the main sequence as $B - V = 0.16$, among the middle-A stars (Simon & Landsman 1997). Farther up the main sequence, weak emission in the near-UV lines becomes much more difficult to detect against an increasingly bright stellar continuum. To extend the search to higher masses it is necessary to look to shorter wavelengths where the photosphere of an A star normally appears much darker. Spectra at UV wavelengths shortward of $\text{Ly } \alpha$ have been obtained for a handful of middle- and early-A stars by the *Far Ultraviolet Spectroscopic Explorer (FUSE)* spacecraft (Simon et al. 2002). The observations suggest a possible sharp cut-off in chromospheric emission and convection zones close to $B - V = 0.12$, near an effective temperature of $T_{\text{eff}} \sim 8300$ K. Although based on a small sample of stars, such a finding is entirely consistent with the predictions of theoretical models for the location of the radiative/convective boundary line in main-sequence stars (Ulmschneider et al. 1996; Christensen-Dalsgaard 2000; Kupka & Montgomery 2002).

There are two significant weaknesses of the conventional stellar envelope models that are worth mentioning here. First, the models generally assume that the transfer of energy by convection in stars with shallow convection zones can be described by standard mixing-length theory; and second, although the chemically normal A-type stars may rotate very rapidly (in some cases close to their critical velocity), the models ignore the potential side-effects of axial rotation. In particular, recent interferometric observations of two rapidly rotating, spin-flattened stars, Altair and α Cep, provide evidence for a difference of almost 2000 K between the surface temperatures at equatorial latitudes and those at the poles (van Belle et al. 2001, 2006; Peterson et al. 2006). Consequently, the outer envelope of a rapidly rotating star may become substantially convective in its cooler equatorial regions while its hotter polar regions remain completely radiative. Recent theoretical models by MacGregor et al. (2007) show the same sorts of structural effects from rapid rotation, forming a deeper convective envelope with increasing rotation. Thus, the notion of a distinct spectral-type or mass-based “dividing-line” between the main-sequence stars that have radiative envelopes and those that have convective envelopes may apply (in a statistical sense) only to the stars that rotate below a certain angular-velocity threshold.

A small minority of normal A stars in the field and in nearby open clusters have also been identified as coronal soft X-ray sources. Cluster A stars have been detected by *ROSAT*

in deep surveys of the Pleiades (Stauffer et al. 1994), the Alpha Persei cluster (Prosser et al. 1996), and the Hyades (Stern et al. 1995), in a few instances at luminosities as high as $L_X \approx 10^{30}$ erg s $^{-1}$. By comparison, the coronae of most (single) late-type stars in the neighborhood of the Sun, including the Sun itself, radiate much less than $\sim 10^{29.3}$ erg s $^{-1}$ in soft X rays (Maggio et al. 1987; Schmitt et al. 1995; Hünsch et al. 1998). Because the majority of cluster A stars are undetected in X rays, the emission of the detected stars could originate not from the A stars themselves, but from hidden late-type binary companions or from unrelated neighboring stars that happen to fall within the X-ray beam. Long pointed observations with *Einstein* and short scans made during the *ROSAT* All Sky Survey (RASS) of ostensibly single A stars or late-B stars in the field have also yielded a number of strong detections (Schmitt et al. 1985; Simon et al. 1995; Berghöfer et al. 1996, 1997; Hünsch et al. 1998). Follow-up observations obtained at higher spatial resolution using the HRI camera on *ROSAT* (Berghöfer & Schmitt 1994) or the ACIS camera on *Chandra* (Stelzer et al. 2003) have confirmed the A or B star is coincident with the X-ray source in some cases, but in other cases have shown that the X rays come from a nearby star while the A or B star appears totally dark in X rays. We note, of course, that even when the positions of the X-ray source and the A or B star closely agree, the identity of the source may not be determined with complete assurance, since it is normally difficult (if not impossible) to prove from an X-ray image alone that the emission is intrinsic to the A or B star and not from an unknown or unresolved (possibly spectroscopic) binary companion.

As one of the central predictions of the stellar structure models, the location along the main sequence where convective envelopes give way to radiative envelopes offers an important observational test of the physical models of main-sequence stars. At present, the two most commonly-used proxies for convection in stars give conflicting results for the location of that transformation, which need to be reconciled: the far-UV observations of chromospheric activity place the transition among the middle-A stars, whereas the X-ray observations of coronal emission place it distinctly farther up the main sequence, among the very early-A or late-B stars. It is essential to determine whether the radiative/convective boundary has been correctly identified by the UV observations or by the X-ray observations. However, observations of the chromospheric lines, which require spectra from *FUSE*, have thus far been limited to a very small sample of A stars. The present study was therefore undertaken to extend the previous *FUSE* survey, and it doubles the size of the sample over the critical range in $B-V$ color and effective temperature where convection, and hence both chromospheric and coronal emission, are expected to vanish. Our main observational goal was to measure accurate fluxes for the high-temperature subcoronal emission lines or to set stringent upper limits on the strengths of those lines.

2. OBSERVATIONS AND EMISSION LINE PROFILE MEASUREMENTS

2.1. Target Selection

Our sample is comprised of 14 main-sequence A stars. All of the stars have $B-V$ colors in the range from 0.23 to 0.01 and optical spectra that are indicative of normal chemical abundances. A list of the stars observed with *FUSE* can be found in Table 1. A journal of the *FUSE* observations is provided in Table 2. Seven stars from this sample were observed in the cycle 1 Guest Observer (G.O.) program of Simon et al. (2002). Those data, denoted in Table 2 by the prefix A041, have been reprocessed here with updated calibration software (CalFUSE 3.1.3). The spectrum of δ Vel was obtained from the cycle 5 G.O. program of Cheng and Neff (Program ID E075). The remaining six stars were observed by us in cycle 3 (Program ID C038) and are reported here for the first time. Following the failure of a reaction wheel on *FUSE*, which limited the declination range that could be accessed by the spacecraft, we observed two additional A-type stars, σ Ara and ν Lup, which were chosen to replace stars on our original target list. However, the bolometric luminosities of both replacement targets were subsequently determined to be much higher than those of the other 14 stars in our sample, and consequently they are omitted from the discussion that follows.

We summarize the relevant parameters of all 14 *FUSE* targets in Table 1. The spectral types, photometry, and parallaxes were extracted from the SIMBAD database. The projected rotational velocities are from the published literature, in most cases from the papers of Abt & Morrell (1995) and Royer et al. (2002a,b). The rotational velocity of α Cep is from the interferometry analysis of van Belle et al. (2006), which yields a larger value than those given by Abt & Morrell (1995) and Royer et al. (2002b), who employed a more conventional approach. The effective temperatures cited for each star were derived from four-color photometry using the “uvbybeta” procedure from the IDL Astronomy User’s Library (Landsman 1993),² which follows the precepts of Moon & Dworetzky (1985). Our T_{eff} estimates are generally within a few hundred kelvins of the values that were derived independently by Allende Prieto & Lambert (1999) from stellar evolutionary calculations and those that were obtained by Sokolov (1995) from the slope of the Balmer continuum between 3200 Å and 3600 Å. The dispersion in temperature for individual stars is comparable to the random scatter of approximately ± 250 K found by Smalley et al. (2002) in the T_{eff} values that were determined for a select group of A stars by a variety of techniques, including the Infra-Red Flux Method (IRFM), four-color photometry, Balmer spectral line profile fitting,

²<http://idlastro.gsfc.nasa.gov/>

and fundamental measurements.

The X-ray luminosities listed in Table 1 are from the *Einstein Observatory* measurements of Schmitt et al. (1985), the RASS catalog of Hünsch et al. (1998), and the analysis of a number of pointed observations obtained from the *ROSAT* archives by Simon et al. (2002). The L_X value for HD 129791 is based on our reductions and XSPEC³ modeling of a 6.3 ks *Chandra* observation of that star, which we obtained from the public archives (ObsID 627; J. L. Linsky, Principal Investigator). HD 129791 is a wide visual binary (CCDM 14460–4452) with a separation of $35''$ that is easily resolved by the ACIS camera on-board *Chandra*. Both the early-type primary star and its much fainter distant companion (CD-44°9590B) were detected in X-rays (the secondary at $L_X = 10^{29.54}$ erg s^{−1}). The other stars were X-ray selected with an a priori bias toward high activity levels so as to favor the detection of high-temperature emission lines. They were designated as X-ray sources by Hünsch et al. (1998), who list all of the main-sequence and subgiant stars from the Yale Bright Star Catalog that can be identified with likely X-ray counterparts in the RASS survey. The angular offset between the optical and X-ray positions for each A star is $\lesssim 10''$, which corresponds to less than one-third the instrumental width of the PSPC camera aboard *ROSAT*. Thus, the association of the X-ray source with the A star instead of a widely separated companion or a physically unrelated neighbor is very likely, but by no means definitive, as cautionary experience with *Chandra* imaging of several *ROSAT* detected late-B stars has already shown (Stelzer et al. 2003). The RASS X-ray luminosities, along with the *Chandra* luminosity we determined for HD 129791, $L_X \gtrsim 1 \times 10^{30}$ erg s^{−1}, make all of our *FUSE* target stars much more active in X rays than the Sun (median $L_X = 10^{27.3}$ erg s^{−1}; Judge et al. 2003) and, indeed, more active than every star in the young Hyades cluster but three (Stern et al. 1995).

We used SIMBAD as well as the Palomar Sky Survey (POSS) and 2MASS images (Skrutskie et al. 2006) to investigate the binary status of each star in Table 1. Our working assumption is that the UV emission of a bright A star should dominate the light in a *FUSE* spectrum and be less subject to the effects of source confusion from a faint binary companion than is the detection of X-ray emission from an X-ray image. The extent to which that critical assumption is borne out by the *FUSE* observations is discussed below. Two stars in Table 1, HD 127971 and β Leo, are wide visual binaries, having a faint optical companion that is separated by a large enough distance ($35''$ and $40''$, respectively) to ensure that the secondary falls outside the *FUSE* science aperture (LWRS: $30'' \times 30''$). The primaries are thus effectively single. Three other stars in our sample, ω Aur, δ Vel, and ι UMa, are

³The XSPEC spectral analysis software is available from the High Energy Astrophysics Science Archive Research Center (HEASARC) of the NASA Goddard Space Flight Center at <http://heasarc.gsfc.nasa.gov/docs/xanadu/xanadu.html>

noted as close visual binaries in the SIMBAD database. In each case, the binary separation is small enough (5".4, 2".6, and 4".5, respectively) and the secondary star is bright enough ($m_v = 8.1, 5.1$, and 9.5 mags, respectively) that the companion, if it is active, must be considered a possible source of the observed UV and X-ray emission. Finally, two stars in our sample are noted as spectroscopic binaries in SIMBAD. β Ari is a double-lined spectroscopic binary in an eccentric orbit with a 107 day period (Tomkin & Tran 1987). The spectral type and mass of the secondary component are estimated by Tomkin & Tran and also by Pan et al. (1990) to be late F or early G and $\sim 1.2 M_\odot$, respectively. The difference in brightness between the primary and secondary is a factor of 15 or more. The other spectroscopic binary in our sample is ι UMa. The visual secondary, a tight pair of 10th magnitude dM stars (the B and C components of the optical triple) is the spectroscopic binary in this hierarchical system.

2.2. The *FUSE* Pointings

The *FUSE* spacecraft and its instrumentation are described by Moos et al. (2000) and Sahnou et al. (2000). The individual *FUSE* observations listed in Table 2 were all acquired in the normal time-tag mode through the LWRS large science aperture. The raw datasets were processed with version 3.1.3 of the CalFUSE calibration software (Dixon et al. 2007), which included screening the photon lists and adjusting the calibrated spectra to compensate for a variety of instrumental signatures (e.g., to exclude the times of burst events). Two integration times are listed for each star, the first for the full exposure, the second for the nighttime portion of the *FUSE* orbit, which normally experiences a lower level of contamination from terrestrial airglow (Feldman et al. 2001). For each of the four detector segments (LiF 1A, LiF 2B, SiC 1A, and SiC 2B), we used CalFUSE to extract spectra from the “good time intervals” of the individual subexposures. Before co-adding, we compared the subexposures to ensure that there were no “drop-outs” due to light loss out of the aperture. We also searched for evidence of substantial variation from one subexposure to the next. Finally, we constructed light curves from the time-tagged data to search for flare-like variations of the O VI emission. We found no evidence for flaring in any of the exposures. The resulting spectra were aligned in wavelength, co-added, and, being highly oversampled in wavelength, rebinned by 3 pixels to a resolution of $\Delta\lambda = 0.039 \text{ \AA}$ as an aid in measuring the strengths of various emission lines. A coarser binning by 9 pixels was also applied to the co-added data in order to construct a broad UV spectral energy distribution (SED) for each star.

Figure 1 presents composite spectra for the 14 stars in our full *FUSE* sample, arranged

in order of increasing T_{eff} as determined from the four-color photometry. Shown here are the LiF 1A and LiF 2A detector segments, which have been stitched together to display wavelengths from the O VI $\lambda\lambda$ 1032, 1038 doublet to the C III multiplet at 1176 Å, except for a small gap in spectral coverage at 1080–1090 Å. Apart from α Cep, the short pointings for the remaining stars are underexposed in the low-sensitivity SiC channels shortward of the O VI lines, so we have truncated the plots to exclude those wavelengths. The changes in SED from one star to the next are consistent with the ordering in T_{eff} established by the optical photometry, despite some discrepancies with the SIMBAD spectral types (notably for HD 43940, which appears to have too early a spectral type, and HD 11636, or β Ari, which may be assigned a spectral type too late for its effective temperature).

The “cleanest” high-temperature lines in the *FUSE* spectra of chromospherically active late-type stars are normally C III λ 977, O VI λ 1032, and the C III λ 1176 multiplet. O VI λ 1038, the weaker component of the O VI doublet, can be blended with both a terrestrial airglow feature and the redward component of the stellar C II $\lambda\lambda$ 1036, 1037 doublet, as can be seen from inspection of the very high quality spectrum of Capella published by Young et al. (2001). Analysis of a moderately high quality spectrum of the A7 V star Altair (Redfield et al. 2002) suggests similar line blending issues for that star as well. It is quite obvious from Fig. 1 that for most stars the emission in C III λ 1176 is bound to be overwhelmed by bright photospheric continuum. The photospheric continuum is substantially lower at the O VI lines, and the wings of the H I Lyman β line further enhance the contrast between the emission lines and the continuum, particularly for the highest temperature targets in our program. The usefulness of the short wavelength spectra for the great majority of A-star targets in the present study is compromised by low SNR at the C III 977 Å line. Therefore, in the following we focus attention on the O VI features, considering principally the stronger λ 1032 component of the atomic doublet. In solar-type stars, these prominent emission features are thought to form in the transition region at a temperature of $\sim 300,000$ K.

2.3. Measurements of the O VI $\lambda\lambda$ 1032, 1038 Lines

The integrated O VI line fluxes and their associated 90% confidence level errors, or the appropriate flux upper limits, were measured for each star by modeling the emission line profile with a single gaussian component and by fitting both linear and quadratic terms to the underlying continuum. The best fit was determined by χ^2 minimization. The complete fitting routine was implemented by means of customized software, which was written in the Interactive Data Language (IDL), as described by Neff et al. (1989). Strong emission lines

in the *HST* spectra and *FUSE* spectra of late-type stars often show signs of a broad pedestal feature requiring a second gaussian component for a proper fit to the observed line profile (Wood et al. 1997; Ake et al. 2000; Redfield et al. 2002). However, a double gaussian fit demands a much stronger line and a much higher signal-to-noise ratio than was achieved for any of the A stars except α Cep, whose spectra (as we are about to show) show no evidence for extended line wings.

The results of our measurements are presented in Table 3, which lists the integrated line fluxes for both components of the O VI doublet and the C III line, the luminosity of the $\lambda 1032$ line, the normalized ratio of the line luminosity to the bolometric luminosity of the star, and the ratio of the measured HWHM (the half-width at half-maximum brightness) to $v \sin i$. Detailed spectra of the O VI lines are shown in Figure 2. In all but one case, the integrated fluxes were extracted from the LiF 1A segment, since the Fine Error Sensor camera in the LiF1 channel (FES-A) was the primary camera that was most often used for guiding on-orbit prior to July 2005. Observations made after that date, however, used the alternative FES-B camera in the LiF2 focal plane assembly to maintain tracking within the science aperture. Consequently, the fluxes of δ Vel were measured instead from the LiF 2B segment. No corrections have been made to the tabulated line fluxes for interstellar extinction, nor should they be needed for such nearby stars.

The stronger $\lambda 1032$ component of the doublet is clearly detected in 11 of the 14 stars, which range in T_{eff} from 7700 K to as much as 10,000 K. The weaker $\lambda 1038$ component can be measured with confidence in 10 stars. It is expected to be intrinsically half as strong as the short wavelength component of the O VI pair, yet is typically somewhat stronger than that, in part because it is difficult to make an accurate measurement of weak emission features in such lightly exposed spectra as ours, but also because of possible contamination from the nearby C II multiplet. The observed line ratio is particularly discrepant for HD 159312, for which the red component of the doublet is clearly the brighter feature, not only in the LiF 1A segment but also in the LiF 2B segment. The emission is distinctly blueshifted with respect to the nominal wavelength of O VI $\lambda 1038$ and likely is due to $\lambda 1037$ line of C II. The asymmetric profile of the $\lambda 1038$ line of α Cep (see Fig. 2) shows unmistakable evidence for extra emission from C II in that star. The $\lambda 1037.02$ line also appears weakly in emission in the spectrum of β Ari.

For three stars (ι Cen, β Leo, and δ Leo) there was no measurable O VI line flux. Upper limits were determined by fitting a constrained Gaussian with its FWHM set to twice the $v \sin i$ of the star, its central peak fixed to match the largest signal in the immediate vicinity of the O VI lines, and a background level set at approximately the lower envelope of fluctuations in the spectrum at nearby wavelengths. These three stars with only upper limits

are among the optically brightest stars in our sample and are by no means the most distant ones observed. Furthermore, the 13.3 ks integration time for ι Cen is one of the longest exposures of all the A stars, second only to the 53 ks spent observing α Cep. To within the uncertainties, our independent measurements of O VI are in substantial agreement with those of Simon et al. (2002) for the 7 stars that were originally observed by those authors.

2.4. Measurements of the C III 977 Å Lines

Wherever possible, we measured the C III 977Å line from the short-wavelength SiC portion of the (orbital night only) *FUSE* spectra (see Table 3). The peak formation temperature of the solar C III line is $T \sim 80,000$ K, which is appreciably lower than that of O VI. We confirm the previous detections and $\lambda 977$ emission line fluxes of Simon et al. (2002) for α Cep and τ^3 Eri. However, the flux and emission line luminosity of $L(977\text{\AA}) = 3.0 \pm 0.2 \times 10^{27}$ erg s $^{-1}$ that we obtain for β Ari are $\sim 40\%$ higher than the earlier published values. Our *FUSE* observations contribute three new detections of C III: HD 43940, $L(977\text{\AA}) = 9.3 \pm 2.3 \times 10^{27}$ erg s $^{-1}$; ω Aur, $L(977\text{\AA}) = 22.8 \pm 5.7 \times 10^{27}$ erg s $^{-1}$; and 33 Boo, $L(977\text{\AA}) = 5.3 \pm 0.9 \times 10^{27}$ erg s $^{-1}$. The same three stars were also firm detections in O VI.

2.5. Interstellar and Photospheric Absorption Lines

Although the absolute wavelength scale of *FUSE* is not well determined, the relative wavelength scale within a particular detector segment of an observation should be accurate to ± 5 km s $^{-1}$ (Redfield et al. 2002). In order to determine whether the narrow emission lines fall at the wavelength expected for the target stars, we searched the LiF1A/2B spectra for interstellar absorption lines or photospheric absorption lines that could be used to establish the absolute wavelength scale. A significant offset from the A star’s radial velocity would suggest that the emission originates from a companion or foreground star. Because our exposure times were optimized to detect line emission, the continuum was always underexposed (see Fig. 1). Consequently, in no case were we able to identify suitable photospheric absorption lines in the LiF1A/2B spectra.

In several cases, we were able to measure the $\lambda 1036.34$ C II interstellar absorption, but it provided an extra constraint only for δ Vel. For that star, the measured C II wavelength was redshifted by 0.09 Å from the laboratory wavelength, while the measured O VI wavelength was redshifted by 0.11 Å. δ Vel has a measured radial velocity of $+2.2$ km s $^{-1}$, and the velocity of the local interstellar cloud in this line of sight is predicted to be $+1.8$ km s $^{-1}$.

(Lallement & Bertin 1992). Therefore, the O VI emission of δ Vel is centered within 5 km s⁻¹ of the expected wavelength of the A star.

3. Results

3.1. Line Flux v. Effective Temperature

A plot of the normalized O VI λ 1032 luminosity, $\mathcal{R} = L(\text{O VI})/L_{\text{bol}}$, versus T_{eff} is shown for the entire sample of A stars in Figure 3. The points located below the slant line include the seven A-type stars that were originally observed by Simon et al. (2002) and also the late-A star Altair, which is denoted by the diamond symbol; the points situated above that line are the X-ray selected target stars that we have observed. In the way of comparison, the normalized λ 1032 luminosity of the quiet Sun is $\mathcal{R}_{\odot} \approx 10^{-7.1}$ (Simon et al. 2002). The vertical dashed line at $T_{\text{eff}} = 8300$ K represents the radiative/convective boundary line according to the conventional stellar envelope models for main-sequence stars.

It is obvious that the two sub-samples exhibit a striking difference in behavior. On the one hand, the sample observed by Simon et al. shows an abrupt fall-off in line emission precisely at the location of the theoretical boundary line. Upper limits on the normalized luminosities of the stars on the high-temperature side of the boundary are 50 times lower than solar, and 20 times lower than the luminosities of A stars on the low-temperature side. On the other hand, in the X-ray selected group we have observed, emission at the solar level is detected up to the earliest spectral type (i.e., A0 V) and the highest T_{eff} (=10,000 K) within our sample. The detection of O VI in the spectrum of HD 129791, our hottest star, is only moderately significant, a slightly less than 4σ result. However, as is clear from Fig. 2, there is no question that O VI emission is present in the spectrum of 33 Boo, which is just slightly later in spectral type (A1 V) and just a bit cooler in T_{eff} (9630 K) than HD 129791. Moreover, as we noted in the previous section, 33 Boo was also detected in C III λ 977 (at approximately half the solar normalized C III luminosity), which confirms the apparent activity of this star.

3.2. UV Flux v. X-Ray Flux

The tight correlation between coronal X-ray emission and the strengths of various chromospheric emission lines is well established among stars with spectral types later than F5 (e.g., Ayres et al. 1981). Similarly, for the early A stars in the present study, Figure 4 shows a strong relationship between the O VI line luminosity and X-ray luminosity, and an equally

pronounced trend in the luminosity normalized to L_{bol} . There is no significant difference in this relationship between the stars with $T_{\text{eff}} \leq 8300$ K (open circles in Fig. 4) and those with $T_{\text{eff}} > 8300$ K (filled circles in Fig. 4).

3.3. UV Line Widths v. $v \sin i$

Both Wood et al. (1997) and Redfield et al. (2002) identify the excess broadening of the narrow components in the UV emission line profiles of late-type stars with wave motions or subsonic turbulence in the transition region, and interpret the highly supersonic nonthermal broadening of the wide pedestal features in terms of stellar microflares. The role such mechanisms might play in heating the outer atmosphere remains unclear. A comparison of the decomposition of the Si IV $\lambda 1394$ line profile of α Cen A and the C IV $\lambda 1548$ profile of AU Mic by Wood et al. (1997) with the analysis of the C III $\lambda 977$ and O VI $\lambda 1032$ profiles of those same stars by Redfield et al. (2002) demonstrates that it is much more difficult to establish the presence of broad line wings in *FUSE* spectra than in *HST* spectra. The SNR of our A star spectra is far from adequate for that purpose.

In contrast with the late-type stars, the widths of the O VI lines of the A stars measured here are generally narrower than the $v \sin i$ values of the stars. All but two of the observed velocity half widths of O VI are less than the $v \sin i$ value (see Table 3). If the chromospheric emission covers the star uniformly, we would expect the observed emission line width to be $v \sin i$ (or larger). A line of subrotational width could be produced if the activity were concentrated at high latitudes. Large polar spots are commonly observed in Doppler images of magnetically-active stars (e.g. Strassmeier et al. 2004). On the other hand, we would expect the effective temperature of a rapidly-rotating A star to be higher at high latitudes (e.g. Peterson et al. 2006). If the emission lines arise in the cooler, low-latitude regions, we would expect to see rotationally-broadened emission lines. The narrow emission lines could also arise from a more slowly-rotating binary companion or foreground late-type star. We further discuss this possibility in later sections.

In two cases, α Cep and τ^3 Eri, the widths of the observed line profiles are in excess of the rotational broadening, and the profiles are not well fitted with a single gaussian emission component. The fluxes, line widths, and uncertainties given in Table 3 were determined from a series of multiple gaussian fits and from a numerical integration of the flux above a background fit. The O VI spectrum of α Cep shown in Fig. 2 bears a very close resemblance to the *FUSE* spectrum of Altair (α Aql), which Redfield et al. (2002) interpret as rotationally broadened and limb brightened. The physical parameters of the two stars are also quite similar. As we noted earlier, the prominent blueward asymmetry in the emission profile

of $\lambda 1038$ is attributable to an added contribution from C II. A similar distortion can be seen in the high signal-to-noise spectrum of the O VI line of Altair, which Redfield et al. decompose into separate Gaussian components. The box-like shape of the profiles of both stars is reminiscent of their Si III $\lambda 1206$ line in *HST* spectra (Simon & Landsman 1997). The profile of the $\lambda 1032$ line of τ^3 Eri, a somewhat slower rotator than either Altair or α Cep, exhibits a narrower width but a similar flat-top shape, although clearly at a much lower SNR.

3.4. Line Flux v. $v \sin i$

UV and X-ray emission of a deeply convective late-type star increases with its axial rotation rate except at the very highest rotation speeds, while the emission of a thinly convective late-A or early-F star is entirely independent of its projected rotation speed (Ayres & Linsky 1980; Simon & Fekel 1987; Simon & Landsman 1991). This difference in the behavior of stars earlier and later than spectral type F5 has led to the suggestion that the activity of these two groups of stars may be produced by different mechanisms (Wolff et al. 1986). The X-ray and O VI luminosities or normalized emission luminosities of the early A stars under investigation here likewise show no dependence on $v \sin i$ (cf Tables 1 and 3). Although our sample is relatively small, the range in velocity is fairly wide, from a low value of 70 km s^{-1} to a top value of 280 km s^{-1} .

Consistent with the outcome of earlier studies, we find that both the coronal X-ray luminosity and the normalized X-ray luminosity of the A stars in this work are independent of the stellar rotation rate, $v \sin i$. The same appears to be true of the UV emission in O VI. Therefore, if rapid rotation has the effect of deepening the outer convection zone of A stars, as suggested by the interferometric observations of Altair and α Cep (e.g., van Belle et al. 2001, 2006) and also by the stellar models of MacGregor et al. (2007), and of promoting the formation of a convectively heated chromosphere or corona, we can point to no empirical evidence for that effect in the observations presented here. At the same time, if the activity of the A stars is powered by a shear dynamo that operates in the largely radiative portions of the envelopes of these A stars, as proposed by MacDonald & Mullan (2004) for the O and B stars, we would again expect to find a trend of increasing X-ray and UV emission with increasing rotation rate, which is not evident in our results.

4. Discussion

The possibility remains that the X-ray as well as the UV emission we observe from the A stars is produced by unrecognized and heretofore undetected companion stars. One example of such possible source confusion is provided by the active Hyades F star, 71 Tau (HD 28052), whose chromospherically active companion was discovered in near-UV emission lines only by virtue of the high spatial resolution of *HST* (Simon & Ayres 2000). Inspection of Fig. 2 and Table 3 suggests that relatively narrow UV emission lines predominate over the obviously rotationally-broadened profiles of α Cep and τ^3 Eri, suggesting that the narrow emission features may originate not from the A stars but from more slowly rotating late-type companions. Consider, for example, the 9 stars with T_{eff} values hotter than 8300 K. ι Cen and β Leo lack O VI emission, and the measurement of HD 159312 is uncertain because only the $\lambda 1032$ line of O VI was detected (the $\lambda 1038$ line was likely obscured by C II emission). Of the remaining 6 stars, only HD 129791, an extremely rapid rotator like α Cep, has broad lines, and in that case the evidence is not definitive because the line emission is weak and the observation is underexposed. The remaining five stars (33 Boo, ω Aur, δ Vel, ρ Oct, and β Ari) all have narrow UV lines, of which three (ω Aur, δ Vel, and β Ari) are already known to have close optical or spectroscopic companions.

Any hidden low-mass secondary able to produce the powerful coronal emission of the X-ray selected A stars we have observed with *FUSE* would have to be counted among the most active late-type stars in the solar neighborhood. For simplicity, we will assume in the following discussion that any such active secondary is a very cool dwarf, either a dK or a dM star. Young, rapidly rotating F and G dwarfs are also known to have X-ray luminosities as high as 10^{30} erg s $^{-1}$, but owing to their higher mass would most likely have made their presence known by inducing radial velocity variations in the spectrum of the primary. As exemplars of possible active secondaries, we choose AB Dor, a rapidly rotating early K dwarf ($v \sin i = 80$ km s $^{-1}$; Zuckerman et al. 2004), which is the namesake of the AB Dor Moving Group (López-Santiago et al. 2006), and AU Mic, a very young, nearby dM1e star with a dusty disk that is a likely member of the β Pic Moving Group (Barrado y Navascués et al. 1999). Both stars are luminous X-ray sources (García-Alvarez et al. 2005; Hünsch et al. 1999), with $L_X \approx 10^{30}$ erg s $^{-1}$, and also strong sources at ultraviolet wavelengths (Wood et al. 1997; Ake et al. 2000; Redfield et al. 2002). The O VI fluxes and emission line luminosities of both stars are listed in Table 3 (original data from Redfield et al. 2002).

The UV emission line luminosities of AB Dor and AU Mic are a suitable match to the $L(\text{O VI})$ values of the active A stars that we have observed with *FUSE* in all but 3 cases. The $L(\text{O VI})$ values for HD 129791 and ρ Oct are unquestionably on the high side, but the SNR in the spectrum of HD 129791 is quite modest and the detection of its O VI emission

is far from the most secure one in our survey. The O VI luminosity of ι UMa, a known binary and a star that is on the convective side of the radiative/convective boundary, is considerably weaker than that of either AB Dor or AU Mic. Instead, it is much more similar to the luminosity of the moderately active K2 V star ϵ Eri, to which Redfield et al. (2002) assigned a flux that is equivalent to $L(\text{O VI}) \approx 5 \times 10^{26} \text{ erg s}^{-1}$. The X-ray luminosities of the two stars are also very similar, $L_X = 10^{28.4} \text{ erg s}^{-1}$ for ι UMa and $L_X = 10^{28.3} \text{ erg s}^{-1}$ for ϵ Eri (Hünsch et al. 1998). There is currently no reason to believe that a star as cool as the A star primary in ι UMa cannot support a chromosphere as well as a corona, but if the high-energy emission observed in this system does come from a companion star, then the secondary (or the secondaries) needs to be mildly but not excessively active.

The foregoing results are summarized in Table 4 in the form of a “truth table.” A check mark next to the name of a star signifies that the proposition stated at the head of a column is TRUE, otherwise it is FALSE or not determinable from the available data. If we exclude both α Cep and τ^3 Eri, for which there is little doubt that the X-ray and UV activity is intrinsic to the A star, the detection of strong X-ray emission that is consistent with an active dK/dM star then appears to be a sufficient condition for the presence of UV emission at an intensity level that is also expected for a dK/dM star; moreover, with but one exception (i.e., β Ari, which is a known binary), it is also a necessary condition.

The commonality of the narrow UV line widths is suggestive of a binary origin of the observed emission, but is not conclusive. Narrow lines could also arise from a high-latitude distribution of active regions, perhaps related to polar spots often seen in the photospheres of active, late-type stars. A further clue as to the origin of the emission can be found, however, in a comparison of the X-ray luminosity with the O VI luminosity. The ratio of the two, $L_X/L(\text{O VI})$, serves as a rough gauge of the differential emission measure between the middle chromosphere and the corona, and is known to be much larger for an extremely active star like AB Dor or AU Mic than for a low-activity star like the Sun. For the former the ratio is ~ 130 and ~ 225 , respectively; for the Quiet Sun it is ~ 5 ; and for a late A-type star like Altair, which is an example of a higher-than-solar mass star with an “X-ray deficit” (Simon & Drake 1989), it is ~ 1 . Among the 9 hottest stars in our sample of A stars whose effective temperatures formally place them above the radiative/convective dividing line at 8300 K, six have supersolar $L_X/L(\text{O VI})$ ratios in the range of 25–160, only one of them (the double-line spectroscopic binary β Ari) has a solar or subsolar ratio, and two (ι Cen and β Leo) have only upper limits in both values and hence an indeterminate X-ray-to-UV luminosity ratio. Among the 5 stars with $T_{\text{eff}} < 8300 \text{ K}$, two have supersolar ratios (HD 43940, 235; ι UMa, 30), two others have solar or subsolar ones (τ^3 Eri and α Cep), and one has dual upper limits and thus an undefined ratio (δ Leo).

5. Conclusions

Of our 14 main-sequence A-type stars, 11 exhibit detectable O VI emission, while restrictive upper limits were determined for the other 3 stars. The stars with O VI span the entire range of T_{eff} , including the range above the presumed convective/radiative “dividing line” around 8300 K. If this sample is representative, and if the emission indeed arises from the A star, then current models of stellar activity must be revised to explain magnetic activity in stars without a substantial convective zone. However, we present several lines of evidence that lead to the conclusion that the emission from the higher-temperature stars in our sample is more likely due to very active late-type dwarf binary companions. The results of our expanded sample are therefore consistent with the observational findings of Simon et al. (2002), which demonstrate a pronounced decrease in UV emission at $T_{\text{eff}} > 8300$ K, and also with the theoretical predictions of the current standard models of stellar structure.

This research has made use of the SIMBAD database, operated at *CDS*, Strasbourg, France, and is based in part on observations from the public archives of the *Chandra X-Ray Observatory*. J.N. acknowledges support by NASA grant NNG04GK80G through the *FUSE* guest observer program to the College of Charleston. T.S. acknowledges support by NASA grant NAG5-12198 through the *FUSE* guest observer program to the University of Hawaii.

Facilities: FUSE, CXO (ACIS).

REFERENCES

- Abt, H. A., & Morrell, N. I. 1995, *ApJS*99, 135
- Ake, T. B., et al. 2000, *ApJ*, 538, L87
- Allende Prieto, C., & Lambert, D. L. 1999, *A&A*, 352, 555
- Ayres, T. R., & Linsky, J. L. 1980, *ApJ*, 241, 279
- Ayres, T. R., Marstad, N. C., & Linsky, J. L. 1981, *ApJ*, 247, 545
- Barrado y Navascués, D., Stauffer, J. R., Song, I., & Caillault, J.-P. 1999, *ApJ*, 520, L123
- Berghöfer, T. W., & Schmitt, J. H. M. M. 1994, *A&A*, 292, L5
- Berghöfer, T. W., Schmitt, J. H. M. M., & Cassinelli, J. P. 1996, *A&AS*, 118, 481
- Berghöfer, T. W., Schmitt, J. H. M. M., Danner, R., & Cassinelli, J. P. 1997, *A&A*, 322, 167
- Browning, M. K., Brun, A. S., & Toomre, J. 2004, *ApJ*, 601, 512
- Brun, A. S., Browning, M. K., & Toomre, J. 2005, *ApJ*, 629, 461

- Christensen-Dalsgaard, J. 2000, in ASP Conf. Ser. 210, Delta Scuti and Related Stars, ed. M. Breger & M. H. Montgomery (San Francisco: ASP), p. 187
- Dixon, W. V., et al. 2007, PASP, 119, 527
- Feldman, P. D., Sahnou, D. J., Kruk, J. W., Murphy, E. M., & Moos, H. W. 2001, J. Geophys. Res. A, 106, 8119
- García-Alvarez, D., Drake, J. J., Lin, L. W., Kashyap, V. Y., & Ball, B. 2005, ApJ, 621, 1009
- Hünsch, M., Schmitt, J. H. M. M., & Voges, W. 1998, A&AS, 132, 155
- Hünsch, M., Schmitt, J. H. M. M., Sterzik, M. F., & Voges, W. 1999, A&AS, 135, 319
- Judge, P. G., Soloman, S. C., & Ayres, T. R. 2003, ApJ, 593, 534
- Kupka, F., & Montgomery, M. H. 2002, MNRAS, 330, L6
- Lallement, R., & Bertin, P. 1992, A&A, 266, 479
- Landsman, W. B. 1993, in ASP Conf. Ser. 52, Astronomical Data Analysis Software and Systems II, ed. R. J. Hanisch, R. J. V. Brissenden, & J. Barnes (San Francisco: ASP), p. 246.
- López-Santiago, J., Montes, D., Crespo-Chacón, I., & Fernández-Figueroa, M. J. 2006, ApJ, 643, 1160
- MacDonald, J., & Mullan, D. J. 2004, MNRAS, 348, 702
- MacGregor, K. B., & Cassinelli, J. P. 2003, ApJ, 586, 480
- MacGregor, K. B., Jackson, S., Skumanich, A., & Metcalfe, T. S. 2007, ApJ, 663, 560
- Maggio, A., Sciortino, S., Vaiana, G. S., Majer, P., Bookbinder, J., Golub, L., Harnden, F. R., Jr., & Rosner, R. 1987, ApJ, 315, 687
- Moon, T. T., & Dworetzky, M. M. 1985, MNRAS, 217, 305
- Moos, H. W., et al. 2000, ApJ, 538, L1
- Neff, J. E., Walter, F. M., Rodono, M., & Linsky, J. L. 1989, A&A, 215, 79
- Pan, X. P., Shao, M., Colavita, M. M., Mozurkewich, D., Simon, R. S., & Johnston, K. J. 1990, ApJ, 356, 641
- Peterson, D. M., et al. 2006, ApJ, 636, 1087
- Pevtsov, A. A., et al. 2003, ApJ, 598, 1387
- Prosser, C. F., Randich, S., Stauffer, J. R., Schmitt, J. H. M. M., & Simon, T. 1996, AJ, 112, 1570

- Redfield, S., Linsky, J. L., Ake, T. B., Ayres, T. R., Dupree, A. K., Robinson, R. D., Wood, B. E., & Young, P. R. 2002, *ApJ*, 581, 626
- Royer, F., Gerbaldi, M., Faraggiana, R., & Gomez, A. E. 2002a, *A&A*, 381, 105
- Royer, F., Grenier, S., Baylac, M.-O., Gomez, A. E., & Zorec, J. 2002b, *A&A*, 393, 897
- Sahnou, D. J., et al. 2000, *ApJ*, 538, L7
- Schmitt, J. H. H. M., Fleming, T. A., & Giampapa, M. S. 1995, *ApJ*, 450, 392
- Schmitt, J. H. M. M., Golub, L., Harnden, Jr., F. R., Maxson, C. W., Rosner, R., & Vaiana, G. 1985, *ApJ*, 290, 307
- Simon, T., & Ayres, T. R. 2000, *ApJ*, 539, 325
- Simon, T., Ayres, T. R., Redfield, S., Linsky, J. L. 2002, *ApJ*, 579, 800
- Simon, T., & Drake, S. A. 1989, *ApJ*, 346, 303
- Simon, T., Drake, S. A., & Kim, P. D. 1995, *PASP*, 107, 1034
- Simon, T. & Fekel, F. C., Jr. 1987, *ApJ*, 316, 434
- Simon, T., & Landsman, W. B. 1991, *ApJ*, 380, 200
- . 1997, *ApJ*, 483, 435
- Skrutskie, M. F., et al. 2006, *AJ*, 131, 1163
- Smalley, B., Gardiner, R. B., Kupka, F., & Bessell, M. S. 2002, *A&A*, 395, 601
- Sokolov, N. A. 1995, *A&AS*, 110, 553
- Stauffer, J. R., Caillault, J.-P., Gagné, M., Prosser, C. F., & Hartmann, L. W. 1994, *ApJS*, 91, 625
- Stelzer, B., Huélamo, N., Hubrig, S., Zinnecker, H., & Micela, G. 2003, *A&A*, 407, 1067
- Stern, R. A., Schmitt, J. H., M. M., & Kahabka, P. T. 1995, *ApJ*, 448, 683
- Strassmeier, K.G. 2002, *AN*, 323, 309
- Tomkin, J., & Tran, H. 1987, *AJ*, 94, 1664
- Ulmschneider, P., Theurer, J., & Musielak, Z. E. 1996, *A&A*, 315, 212
- van Belle, G. T., Ciardi, D. R., Thompson, R. R., Akeson, R. L., & Lada, E. L. 2001, *ApJ*, 559, 1155
- van Belle, G. T., et al. 2006, *ApJ*, 637, 494
- Wolff, S. C., Boesgaard, A. M., & Simon, T. 1986, *ApJ*, 310, 360
- Wood, B. E., Linsky, J. L., & Ayres, T. R. 1997, *ApJ*, 478, 745

Young, P.R., Dupree, A. K., Wood, B. E., Redfield, S., Linsky, J. L., Ake, T. B., & Moos, H. W. 2001, *ApJ*, 555, L121

Zuckerman, B., Song, I., & Bessell, M. S. 2004, *ApJ*, 613, L65

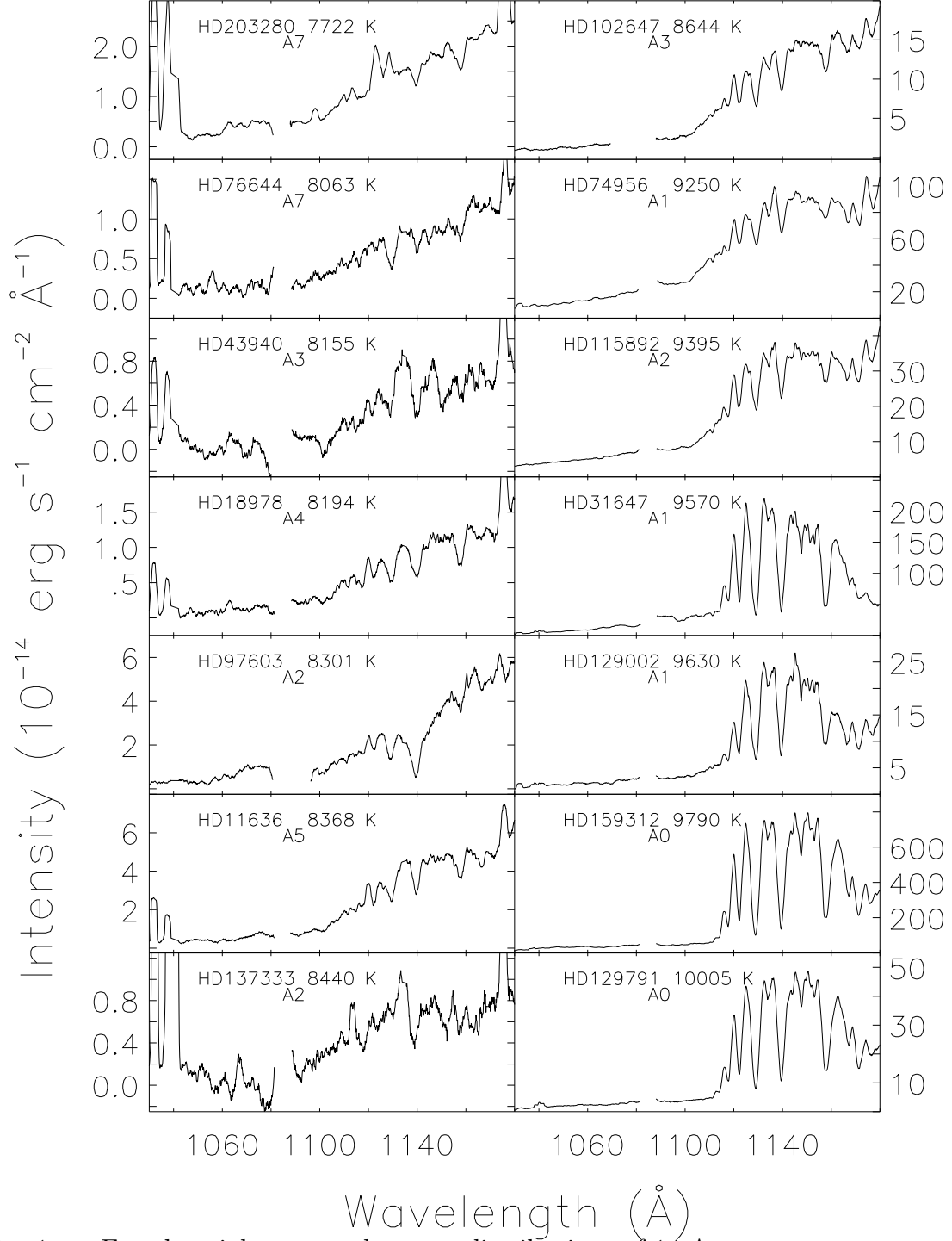


Fig. 1.— Far-ultraviolet spectral energy distributions of 14 A-type stars.

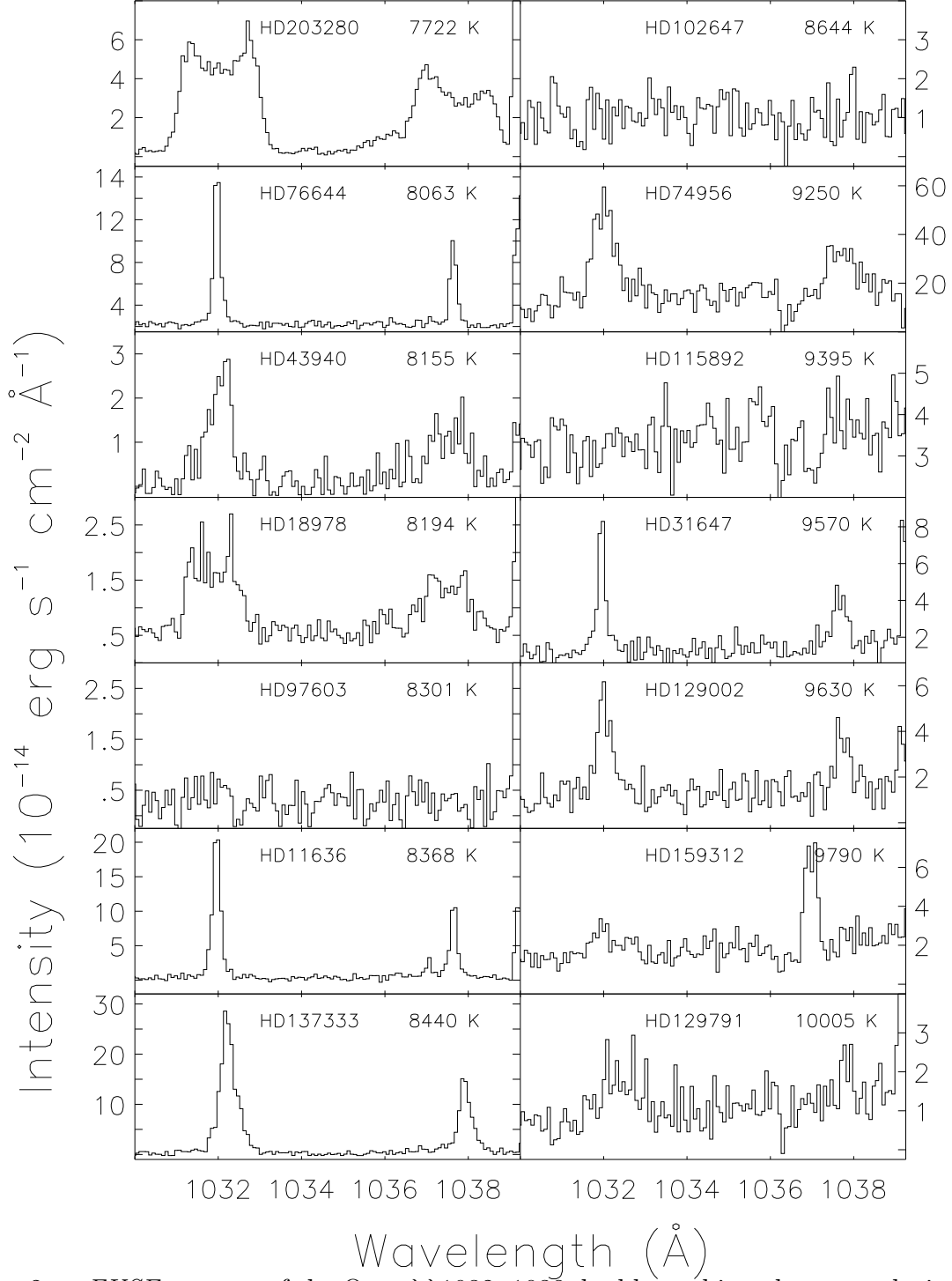


Fig. 2.— *FUSE* spectra of the O VI $\lambda\lambda 1032, 1038$ doublet, rebinned to a resolution of 0.04 \AA per pixel. O VI emission was detected in 11 of the 14 stars. Except for HD203280 and HD18978, the O VI emission lines are narrower than expected from the star’s $v \sin i$.

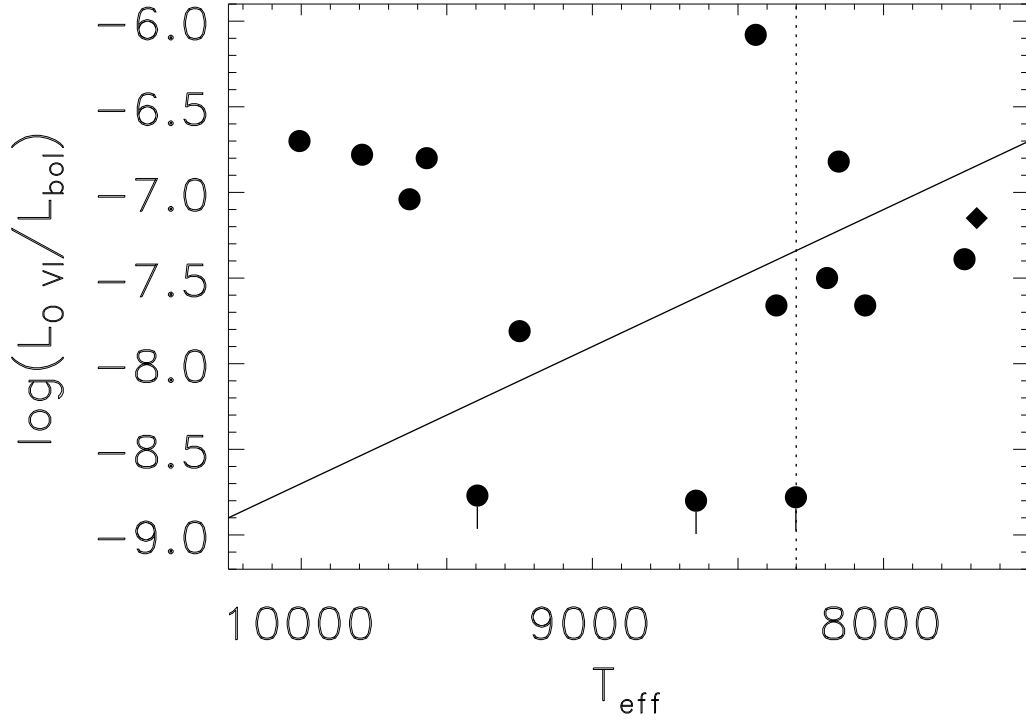


Fig. 3.— Measured O VI emission line luminosity, normalized to the bolometric luminosity, plotted as a function of T_{eff} . *Filled Circles*: A-type stars observed or re-measured in this survey. Three of these are plotted as upper limits. The circled points lying below the solid line were originally observed by Simon et al. 2002. *Diamond*: the A7 star Altair, data from Redfield et al. 2002. The vertical dotted line at $T_{\text{eff}} = 8300$ is a hypothetical boundary line that separates stars with sub-photospheric convective layers from those with purely radiative outer envelopes.

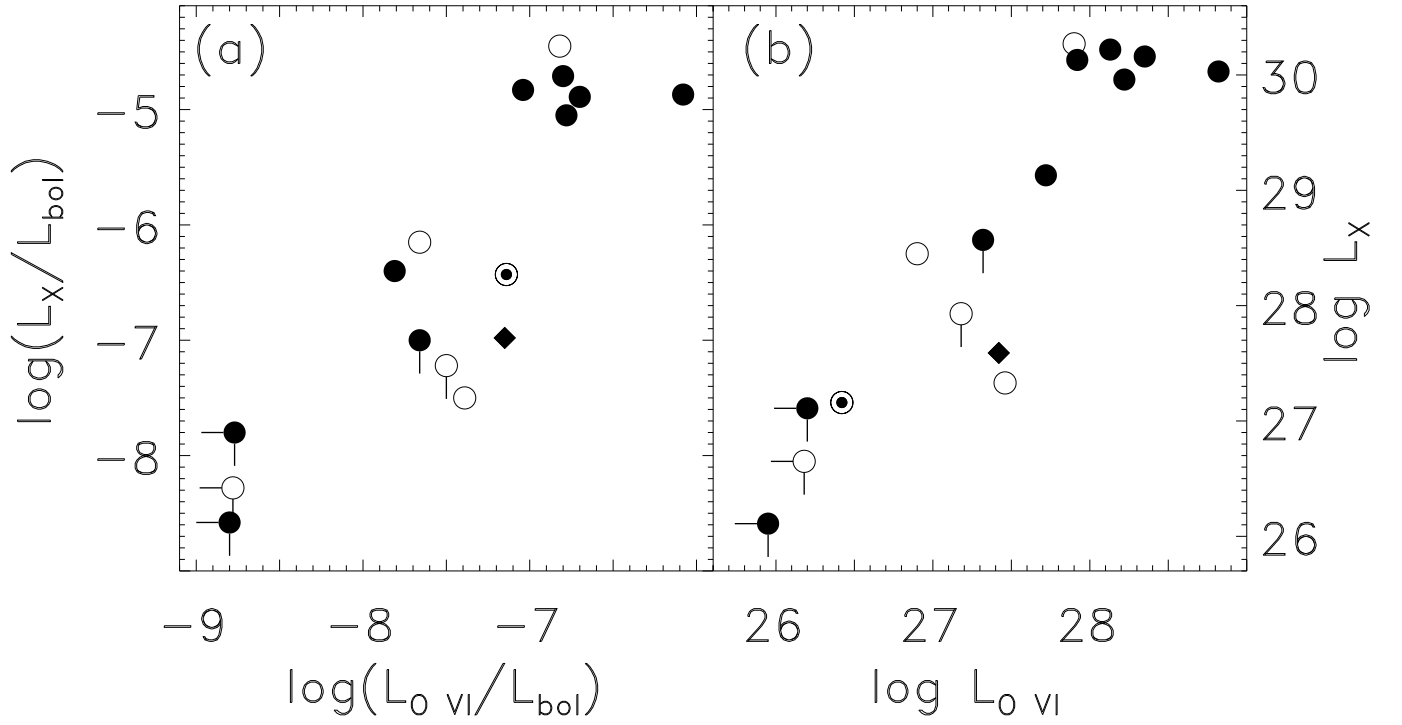


Fig. 4.— (a) Correlation between L_X/L_{bol} and $L(\text{O VI})/L_{\text{bol}}$. Also plotted are the Sun (circled dot) and Altair (diamond symbol). The open circles denote the stars with $T_{\text{eff}} \leq 8300$, i.e., those to the right of the dividing line in Fig. 3. (b) A similar correlation is seen between L_X and $L(\text{O VI})$.

Table 1. Properties of the Stars Observed With *FUSE*

Name	HD	Sp. Ty.	$v \sin i$ (km s ⁻¹)	V	$B-V$	π (mas)	M_v	L_{bol}/L_{\odot}	β	$b-y$	T_{eff} (K)	$\log L_X$ (erg s ⁻¹)	References
HIP 72192 ^a	129791	A0 V	280	6.91	0.05	7.72	1.35	28.9	2.867	0.035	10,000	30.16	4, 5, 10
HR 6539	159312	A0 V	...	6.48	0.01	9.64	1.40	26.4	2.886	-0.005	9790	29.96	2
33 Boo	129002	A1 V	95	5.40	0.03	16.56	1.49	23.6	2.910	0.000	9630	30.13	1, 2, 5
ω Aur ^b	31647	A1 V	110	4.99	0.02	20.50	1.55	22.2	2.900	0.006	9570	30.22	1, 5
ι Cen	115892	A2 V	75	2.70	0.09	55.64	1.43	24.1	2.901	0.004	9395	<27.11	3, 8
δ Vel ^{b, d}	74956	A1 V	150	1.95	0.05	40.90	0.01	87.1	2.876	0.034	9250	29.13	2, 4, 5
β Leo ^a	102647	A3 V	115	2.14	0.09	90.16	1.92	14.0	2.899	0.043	8645	<26.11	1, 5, 6
ρ Oct	137333	A2 V	150	5.58	0.11	15.02	1.46	20.9	2.887	0.072	8440	30.03	2, 3
β Ari ^c	11636	A5 V	70	2.64	0.13	54.74	1.33	23.3	2.879	0.059	8370	<28.57	1, 5, 7
δ Leo	97603	A4 V	180	2.56	0.12	56.52	1.30	23.9	2.869	0.067	8300	<26.65	1, 5, 8
τ^3 Eri	18978	A4 V	120	4.10	0.16	37.85	1.99	12.6	2.858	0.091	8195	<27.93	1, 5, 7
HR 2265	43940	A3 V	250	5.88	0.14	16.10	1.91	13.4	2.853	0.073	8155	30.27	2, 4, 5
ι UMa ^{b, c}	76644	A7 V	140	3.10	0.23	68.32	2.29	9.5	2.843	0.104	8060	28.45	1, 2, 5
α Cep	203280	A7 IV-V	283	2.44	0.22	66.84	1.57	18.2	2.807	0.127	7720	27.33	8, 9

Note. — (a) Wide binary; (b) Close binary; (c) Spectroscopic binary; (d) Eclipsing binary.

References. — (1) Abt & Morrell 1995; (2) Hünch et al. 1998; (3) Levato 1972; (4) Royer et al. 2002a; (5) Royer et al 2002b; (6) Schmitt 1997; (7) Schmitt et al. 1985; (8) Simon et al. 2002; (9) van Belle et al. 2006; (10) This paper.

Table 2. Journal of *FUSE* Observations

Star	<i>FUSE</i> Dataset	UT Date (yyyy-mm-dd)	No. of Subexp.	Exp. Time ^a (ks)	Night Only ^a (ks)
HD 129791	C0380801000	2002-04-24	2	6.3	3.5
HD 159312	C0381201000	2004-09-11	4	9.8	5.6
33 Boo	C0380301000	2002-05-24	2	6.1	4.2
ω Aur	C0380901000	2002-10-09	5	3.6	2.5
ι Cen	A0410505000	2000-07-09	11	13.3	8.7
δ Vel	E0750102000	2006-07-12	2	4.0	3.2
δ Vel	E0750103000	2006-07-15	4	8.3	4.2
β Leo	A0410202000	2001-04-17	7	6.8	3.9
ρ Oct	C0380402000	2002-08-06	3	3.9	0.0
β Ari	A0410101000	2001-09-03	9	10.3	2.8
δ Leo	A0410303000	2000-12-21	9	7.4	1.8
τ^3 Eri	A0410606000	2001-08-06	4	12.6	3.0
HD 43940	C0380101000	2002-11-06	2	5.6	3.7
ι UMa	A0410405000	2001-11-04	2	5.7	1.7
α Cep	A0410707000	2000-08-12	8	27.5	15.0
α Cep	A0410708000	2000-08-12	9	25.8	12.6

^aCumulative accepted exposure times (good time intervals) at the wavelength of O VI.

Table 3. Observed FUV Emission-Line Fluxes

Star	$f(\text{O VI})^{\text{a}}$ 1032 Å	$f(\text{O VI})^{\text{a}}$ 1038 Å	$L(\text{O VI})^{\text{b}}$ 1032 Å	$L(\text{O VI})/L_{\text{bol}}^{\text{c}}$ 1032 Å	$f(\text{C III})^{\text{a}}$ 977 Å	FWHM ^d / $v \sin i$
HD 129791	1.1±0.3	...	22±6	2.0±0.6	...	0.36
HD 159312	1.3±0.1	1.9±0.1 ^e	17±1	1.7±0.1
33 Boo	1.9±0.1	1.1±0.1	8.3±0.4	0.92±0.05	1.2±0.2	0.50
ω Aur	4.7±0.2	2.8±0.2	13±1	1.6±0.1	8.0±2.0	0.27
ι Cen	< 0.4	<0.5	<0.2	<0.02
δ Vel	7.3±0.2	3.8±0.6	5.2±0.1	0.16±0.01	...	0.56
β Leo	< 0.6	<0.4	<0.1	<0.02
ρ Oct	12.4±0.6	5.6±0.8	66±3	8.3±0.4	...	0.43
β Ari	5.2±0.2	2.3±0.2	2.1±0.1	0.22±0.01	7.5±0.5	0.44
δ Leo	< 0.4	<0.2	<0.2	<0.02
τ^3 Eri	1.8±0.1	1.3±0.2	1.5±0.1	0.31±0.02	...	1.40
HD 43940	1.7±0.2	1.2±0.2	7.9±0.9	1.5±0.2	2.0±0.5	0.26
ι UMa	3.1±0.2	1.6±0.1	0.80±0.05	0.22±0.01	...	0.20
α Cep	10.7±0.7	7.3±1.3	2.87±0.19	0.41±0.03	32.5±2.0	1.40
AB Dor ^f	44.9±4.5	<25.4	11.9±1.2	81.5±8.2
AU Mic ^f	20.9±2.4	10.6±1.1	2.5±0.3	53.3±6.1

^aEmission line flux in units of 10^{-14} erg s⁻¹ cm⁻² at Earth, not corrected for interstellar extinction.

^bEmission-line luminosity in units of 10^{27} erg s⁻¹.

^cNormalized O VI λ 1032 luminosity in units of 10^{-7} .

^dRatio of the half-width at half-maximum of O VI 1032 Å, expressed as a velocity, to the stellar $v \sin i$.

^eMost of this is likely due to C II emission; see text.

^f*FUSE* fluxes for AB Dor (K0-1 IV/V) and AU Mic (M1.6 Ve) from Redfield et al. 2002.

Table 4. Comparison of A Stars with Two Active Low-Mass Stars

Star	T_{eff} (K)	Known or Possible Binary	$L_X(A_*) \sim$ $L_X(\text{dK}_*/\text{dM}_*)$	$L_{OVI}(A_*) \sim$ $L_{OVI}(\text{dK}_*/\text{dM}_*)$
HD 129791	10,000	...	✓	✓
HD 159312	9,790	...	✓	✓
33 Boo	9,630	...	✓	✓
ω Aur	9,570	✓	✓	✓
ι Cen	9,395
δ Vel	9,250	✓	✓	✓
β Leo	8,645
ρ Oct	8,440	...	✓	✓
β Ari	8,370	✓	...	✓
δ Leo	8,300
τ^3 Eri	8,195	✓
HD 43940	8,155	...	✓	✓
ι UMa	8,060	✓
α Cep	7,720	✓

Note. — The late-type comparison stars are AB Dor (dK; $T_{\text{eff}} \approx 5200$ K) and AU Mic (dM; $T_{\text{eff}} \approx 3500$ K).